Journal of Constructional Steel Research 187 (2021) 106995

Contents lists available at ScienceDirect

Journal of Constructional Steel Research

journal homepage: www.elsevier.com/locate/jcsr

Design of circular steel flange plates subjected to tension loads – yield line approach

Mohamed A. Khedr [a,b,*]

[a] BC Hydro, Burnaby, BC, Canada
[b] Department of Civil Engineering, Faculty of Engineering, Benha University, Benha, Egypt

ARTICLE INFO

Keywords:
Flange plate
Circular
Bolted
Tension loads
Yield line
Failure mechanism
Finite element
Contact

ABSTRACT

The use of circular steel flange plates with circular bolts pattern connections is common in tubular structures used in different applications such as transmission and communication structures. Several published literatures include methods for the design of these connections under tension loads. These methods are not widely used in the industry as they are either complex or yielding results that are not always consistent with published test data. Therefore, there is still a need for a simplified, yet accurate, method for designing these connections when subjected to tension loads.

This paper presents a numerical study performed on circular flanged connections subjected to concentric axial tension loads. The analysis part of the study is conducted using the Finite Element (FE) package ADINA considering one common geometrical flange plate configuration, ring configuration, while considering contact surface separation. The results obtained from the FE analyses are compared with published experimental data from which it is concluded that the FE model can predict the behaviour of these connections with a high degree of accuracy.

Parametric investigation is then conducted to numerically expand the experimental data to gain more insight into the behaviour of these flange plate connections and to use this data later in this work to validate the proposed design method. The varying parameters considered in the numerical investigation include base plate thickness; number of bolts; bolt circle diameter and plate diameter.

A simple design approach based on yield line theory is then introduced and a comparison between yield loads predicted using the proposed model and the finite element results is presented. The yield loads resulting from proposed design method show good agreement with the finite element results with 10% maximum difference.

1. Introduction

Circular and polygonal hollow structural sections are used in wide range of structural applications such as long span space trusses, traffic signals, sign supports, lighting poles, telecommunication and transmission poles and towers to name a few. The use of tubular members is preferred in these applications due to their aesthetic appearance and lower wind drag coefficients when compared to flat members. It is common to connect the members of these structures together utilizing circular flange plates with circular bolt patterns. These connecting plates are either subjected to axial tension or compression forces as in the case of trusses or latticed towers or subjected to axial forces, shear forces and bending moments as in the case of poles. In detailing theses connections two common configurations are typically used either ring plate with double fillet welds, inner and outer, or blank plate with full penetration weld and outer reinforcement fillet weld.

Connections design in general have been studied extensively and design guidelines are available in design standards and published literature. However, this is not the case with circular flange plate although their use is common as published literature has come short of recommending a simplified design method for proportioning these connections.

One of the first available published articles studying the behaviour of circular plate connections with circular bolt patterns was published in the eighties of the past century Kato and Hirose [9] studied the maximum strength of circular tension flanged joints with high strength bolts. In their work, yield line analysis was used in determining the maximum bending strength of the connecting flange plates when

* Corresponding author.
E-mail address: mohamed.khedr@outlook.com.

https://doi.org/10.1016/j.jcsr.2021.106995
Received 22 July 2021; Received in revised form 7 October 2021; Accepted 8 October 2021

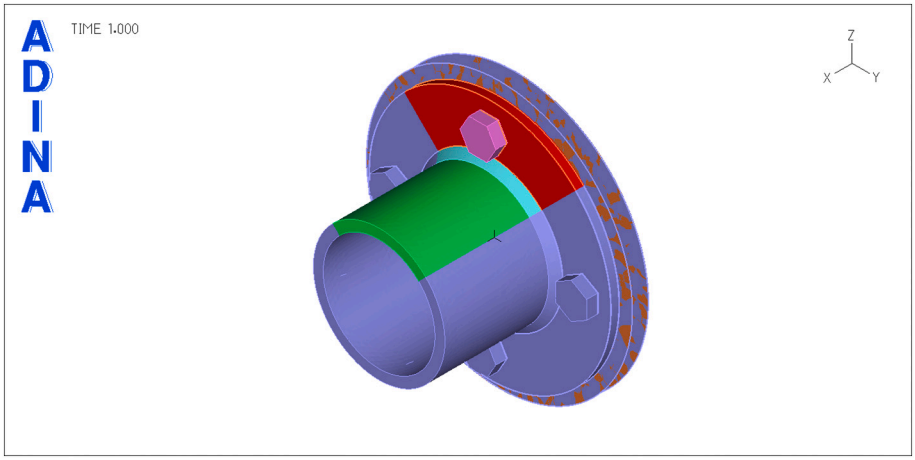

Fig. 1. General view of the 3-D finite element model of the connection.

members are subjected to direct tension loads while considering prying force. The calculated strengths using the proposed yield line model were then compared to results obtained from 63 tests collected from the literature. The accuracy of the proposed method is found to be unsatisfactory as an error margin of more than 100% is reported for some specimens.

In a recent study, Couchaux et al. [20] presented a solution to determine the ultimate tensile resistance of bolted flange connection using yield line that is based on earlier work done by Igarashi et al. The presented work was divided into experimental, finite element analysis then analytical and simplified. The study did not only focus on the yielding of the flange plate and combined yielding of plates and bolts but on all failure mechanisms including failure of the bolt group, pipe, and weld. Only few occurrences of the reported failures were attributed to flange failure, for these occurrences the presented simplified approach significantly underestimated the yield load.

Ghareeb et al. [14] executed a research program to study the behaviour of circular base plates subjected to bending moment. A test program was devised where a total of twelve specimens were tested to failure. In that study, two variables were considered: plate thickness and presence of stiffeners. Other design variables were kept constant throughout the study. A design formula based on yield line approach, which yielded acceptable results, was presented. However, the suggested formula was complicated and not suitable for hand calculations. In a subsequent numerical and analytical study, Khedr and Heikal [7] presented finite element analyses and parametric study followed by a simplified yield line approach for the design of such connections subjected to pure bending.

The current study aims at gaining a better understanding of the behaviour of the circular flanged plate connections under tension load and suggesting a simplified method suitable for designing these connections. Three-dimensional finite element model of the connections under investigation is designed considering material non-linearities and contact separation between the different connection components. The finite element models are verified using published experimental results collected from different test programs. Parametric study is then performed using FE analysis to assess the impact of changing some design parameters on the behaviour of circular flange plate connection. This is followed by suggesting a simple model based on yield line theory to estimate the yield Load and mode of failure of the flange connection.

2. Finite element models

2.1. General

The simulation of the behaviour of the flange connection under investigation is conducted through constructing three-dimensional, 3D, finite element models created and analysed using the general-purpose finite element software ADINA [3]. The finite element models utilize nonlinear material models for the various elements of the connection, bolt elements with pretension load, and contact elements to simulate separation between different surfaces. The next few clauses present in some details the various aspects of the finite element models.

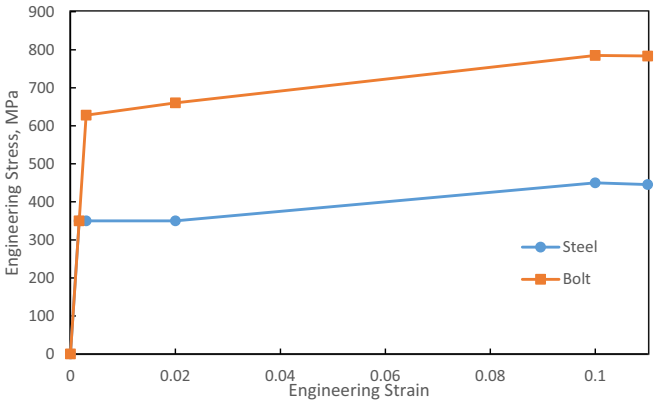

Fig. 2. Sample of the idealized multi-linear steel model used in the FE analyses.

2.2. 3-D steel connection model

The geometry of the 3D models for the connection are created utilizing the solid modular ADINA-M available in the finite element package. Fig. 1 shows the basic connection model consisting of pipe, weld, flange plate, bolts, and rigid contact body.

2.3. Steel material model

An idealized multi-linear stress-strain relation with von-Mises yield criterion and isotropic strain hardening is used in defining the steel material assigned to the main components of the FE model. In defining the engineering stress-strain relation, Fig. 2, four points are evaluated based on the steel material utilized [13,17]. The first point is the yield point which is calculated assuming Young's modulus to be 210 GPa, beyond the yield point a yield plateau is assumed up to a strain of 0.02. This is followed by a strain hardening portion up to the ultimate stress value which is assumed at strain of 0.1 followed by a declining branch till failure.

2.4. Bolt material model

Like steel material model, a multi-linear stress-strain model with von-Mises yield criterion and isotropic strain hardening is used in defining the bolt material as shown in Fig. 2. In this case the engineering stress-strain relation is defined by four points only. The first strain point is corresponding to the yield stress of the bolt material and is calculated assuming Young's modulus to be 210 GPa followed by a strain hardening portion up to the ultimate stress value of 785 MPa which is assumed to occur at strain equals to 0.1 followed by a declining branch till failure.

2.5. Load

A uniform tension load acting in the global X direction is applied normal to the pipe wall. The load is increased incrementally in linear fashion following a time function from zero to full value utilizing the automatic time stepping option in ADINA. It should be noted that in the verification portion of the current work displacement control analyses are performed to simulate the specimens' behaviour in tension till failure.

2.6. Contact pairs and boundary conditions

The model includes three contact pairs as follows:

i. The first contact pair consists of the inside face of bolt head and top face of flange plate where the flange plate is the target.
ii. The second contact pair consists of the bottom face of flange plate and the top face of the rigid body where the flange is considered as the contactor.
iii. The third contact pair consists of the inside face of the nut and bottom face of the rigid body where the nut is considered as the contactor

The translations in the three main orthogonal directions are restrained along the bottom surface of the rigid contact body.

2.7. Tetrahedra elements

The 10-node tetrahedra element with three translational degrees of freedom per node is used to model the flange plate, bolts, weld, and pipe. A minimum of four elements across the thickness of the base plate are used to properly capture the bending behaviour of the plate.

2.8. Bolt element option

To specify the bolt pretension load, bolt option is selected in the bolt element group and the pretension load is specified. The full bolt pretension load is applied to the bolt element group in five equal steps prior to the application of the external load.

2.9. Cyclic symmetry

Due to the symmetric nature of the connection model and the applied load only one slice of the connection, as shown in Fig. 1, is modelled and cyclic symmetry option of the software is utilized to reduce the computation time.

2.10. Analysis assumptions and convergence criteria

Static analysis with large displacements and large strain formulation is used to simulate the actual behaviour of the connection. Due to the non-linear nature of the problem that is present due to the materials non-linearity and the presence of contact surfaces two contact convergence criteria need to be specified these are energy and contact tolerances for which the default values of the software, 1E-03 and 5E-02 respectively, are used.

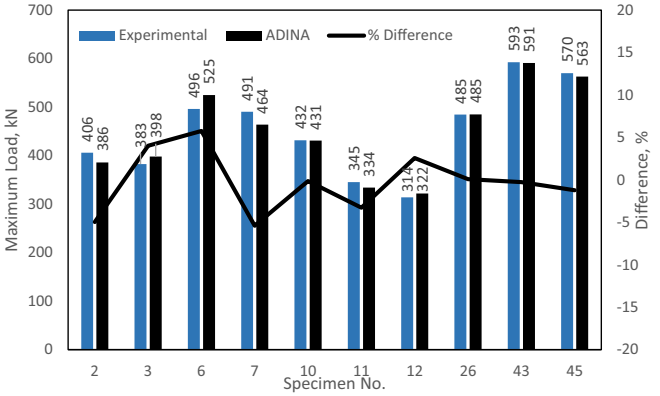

Fig. 3. Comparison between experimental and FE failure load for 10 different connections, [9].

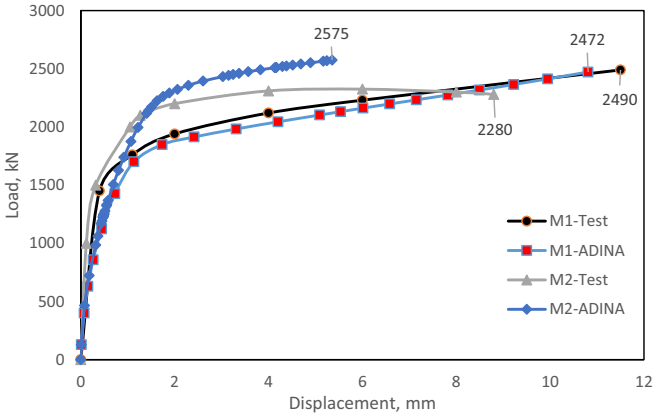

Fig. 4. Comparison between experimental and FE results for M1 and M2 connections [16].

3. Validating the finite element model

3.1. Using experimental results

To validate the finite element model and analysis assumptions it is important ensure that the model can capture the overall behaviour of the tested specimens. Two studies are used in performing this validation Kato and Hirose [9] and Van-Long et al. [16].

The circular flange connection test results reported in Kato and Hirose are used in verifying the assumptions used in developing the current finite element model. It should be noted that although two types of flange connections, ring and blank, were included in their work, only the reported test data for the ring flanged connections are used in the current validation. A total of 53 specimens were tested; three different member sizes were used: 76.2; 114.3 and 168.3 mm in diameter. All specimens were with 6 bolts arranged on circular bolt circle with varying bolt diameter, flange plate thickness, bolt circle and plate diameter. Fig. 3 presents a comparison between the failure loads of 10 of the tested specimens, the numbers on the x-axis refer to the specimen number as reported in the study, and the values obtained from FE simulation. Comparing the FE analyses results to those reported in the study it is found that the FE failure load values are in good agreement with the reported test values with the calculated error found to be between −5% and 6%. The reader is advised to refer to Kato's study for full insight of the tested specimens.

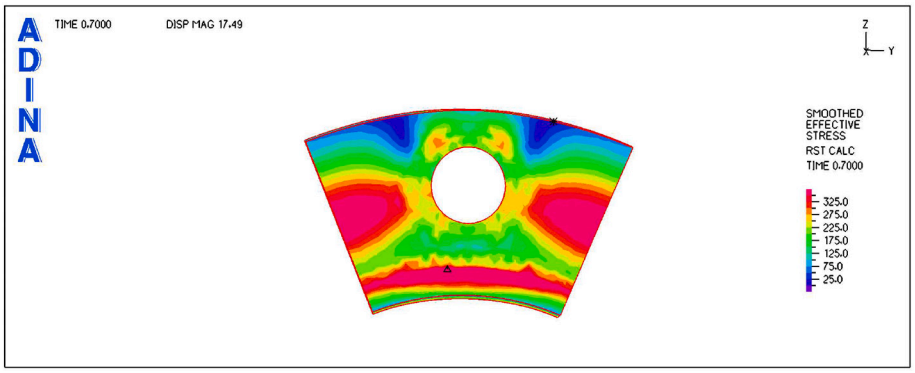

i) Plate Yielding Around Pipe and Bolt Circle

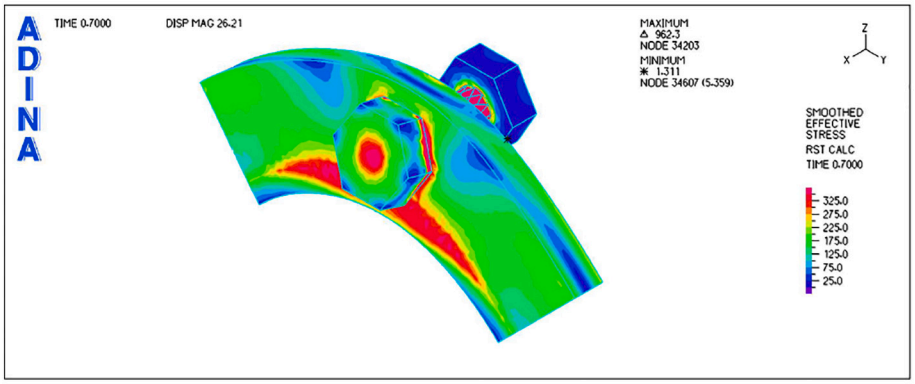

ii) Plate Yielding Around Pipe Associated with Bolt Group Yielding

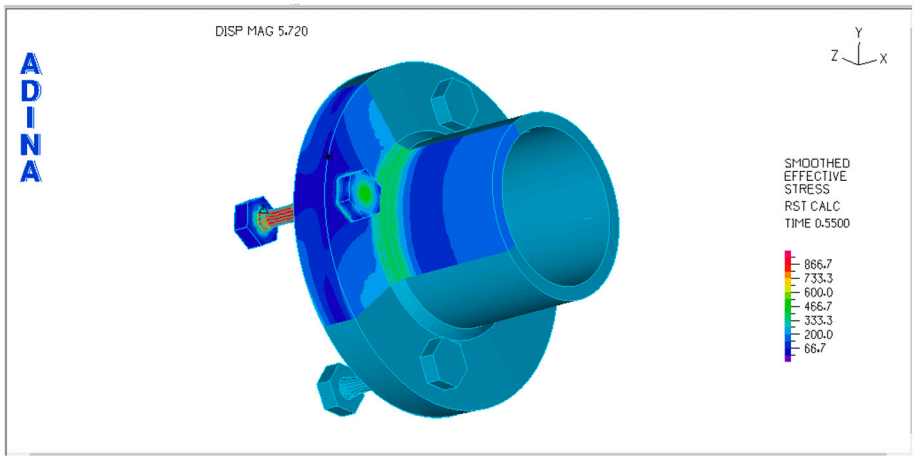

iii) Bolt Group Yielding

Fig. 5. Effective stress distribution associated with different modes of failure.

Van-Long et al. tested specimens consisting of a 356 mm diameter 12 mm thick tube full pen welded to 556 mm diameter blank flange with a reinforced line of fillet weld. The specimens were connected via 12 bolts arranged on bolt circle diameter of 456 mm. Two different configurations were tested under static load. The first configuration, M1, with 15 mm flange thickness and M27 bolts. While the second configuration, M2, with 20 mm thickness and M20 bolt. A complete description of the specimens, materials, bolt pretension etc. can be found in their study. Load displacement response of the tested specimens reported in their work and that of the FE simulation is shown in Fig. 4. Comparing the curves shown in Fig. 4, it is clear that the FE analyses can capture the experimental load displacement behaviour of these specimens with good accuracy. The difference between the failure load as reported in the study and that resulting from the FE analyses is found to be 0% and 13% for M1 and M2 respectively.

3.2. *Simulating different modes of failure*

In analogy with L-Stub theory there are three failure mechanisms that can occur in flange plate connections. These failure mechanisms are

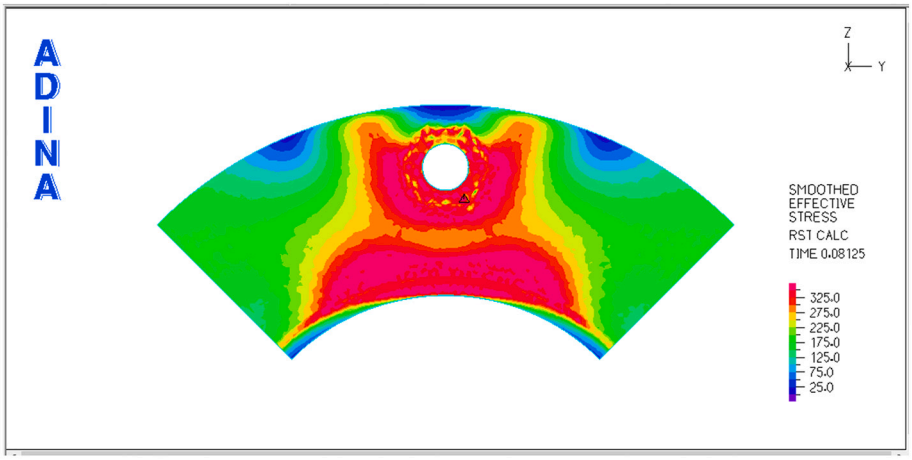

iv) Plate Bolt Zone Yielding

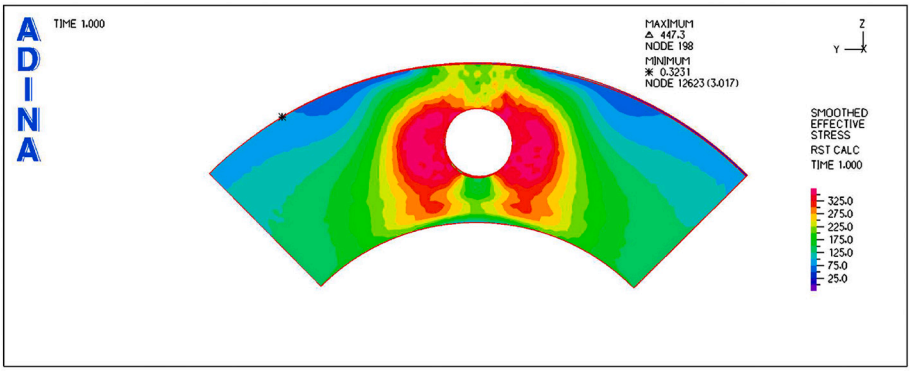

v) Fan Mechanism

Fig. 5. (*continued*).

flange failure; bolts failure; or a combination of both. The relative resistance of the flange and bolts dictates which mode occurs. In case of strong bolt group and thin plate, the failure is due to yielding of the plates, whereas a bolt failure occurs with thick plates and weak group of bolts. There exists an intermediate case where the failure is due to combined failure of the plate and the group of bolts [18].

Re-phrasing the above in the context of the circular flange joints of pipes, failure of this connection type can be described in the following three main failure modes:

Mode 1: Plate yielding around the pipe and along bolt circle.

Mode 2: Plate yielding around the pipe associated with bolt group yielding.

Mode 3: Bolt group yielding.

When the circumferential distance between the bolts is large enough local yield mechanism around the individual bolts may developed [15]. This result in two variations of Modes 1 and 2 as follows:

Mode 4: Yield of the plate around part of the pipe and bolt zone.

Mode 5: Fan mechanism or localized yielding of the plate around bolt only.

It is therefore essential to verify the robustness of the model and ensure that the model can capture the five failure modes listed above. To this end, modes 1 through 5 listed above are simulated through changing the connection design parameters. Resulting connection failure modes and the associated effective stress distributions are shown on Fig. 5. These five failure modes are also presented schematically in Fig. 6 which are used later in the yield line analysis section of this work.

3.3. Bolt pretension load and prying force

To examine the model's capability of accurately predicting the prying force developed in the bolts, a 6″ pipe with 12 mm thick and 315 mm diameter flange plate is modelled. The flange plate is connected via four 5/8″ diameter F3125 grade A325 bolts arranged on 270 mm bolt circle diameter. The pretension load of the bolts is varied between no pretension and full pretension which is assumed at 70% of the ultimate strength of the bolts [2,11].

For each pretension level the applied tension load is varied and the bolt force is calculated and then plotted against the applied load as shown in Fig. 7. From this figure it is evident that the FE model can capture the prying force developed in the bolt as the flange plate deforms and bear against the rigid contact surface. It is worth noting that the prying force, Q, can be determined using this figure as the minimum of the difference between the bolt force and the pretension load, Q_1, and the difference between the bolt force and the applied external force per bolt, Q_2. Fig. 7 shows the developed prying force for the connection with 40 kN pretension load.

4. Parametric study

After verifying the accuracy and robustness of the FE model, the study is extended to perform a parametric investigation to examine the effect of changing several design parameters on the behaviour of the connections to be used later in suggesting a simplified design model for their design.

In planning the parametric study, the pipe diameter is chosen such as to cover a realistic range of the diameters typically used in

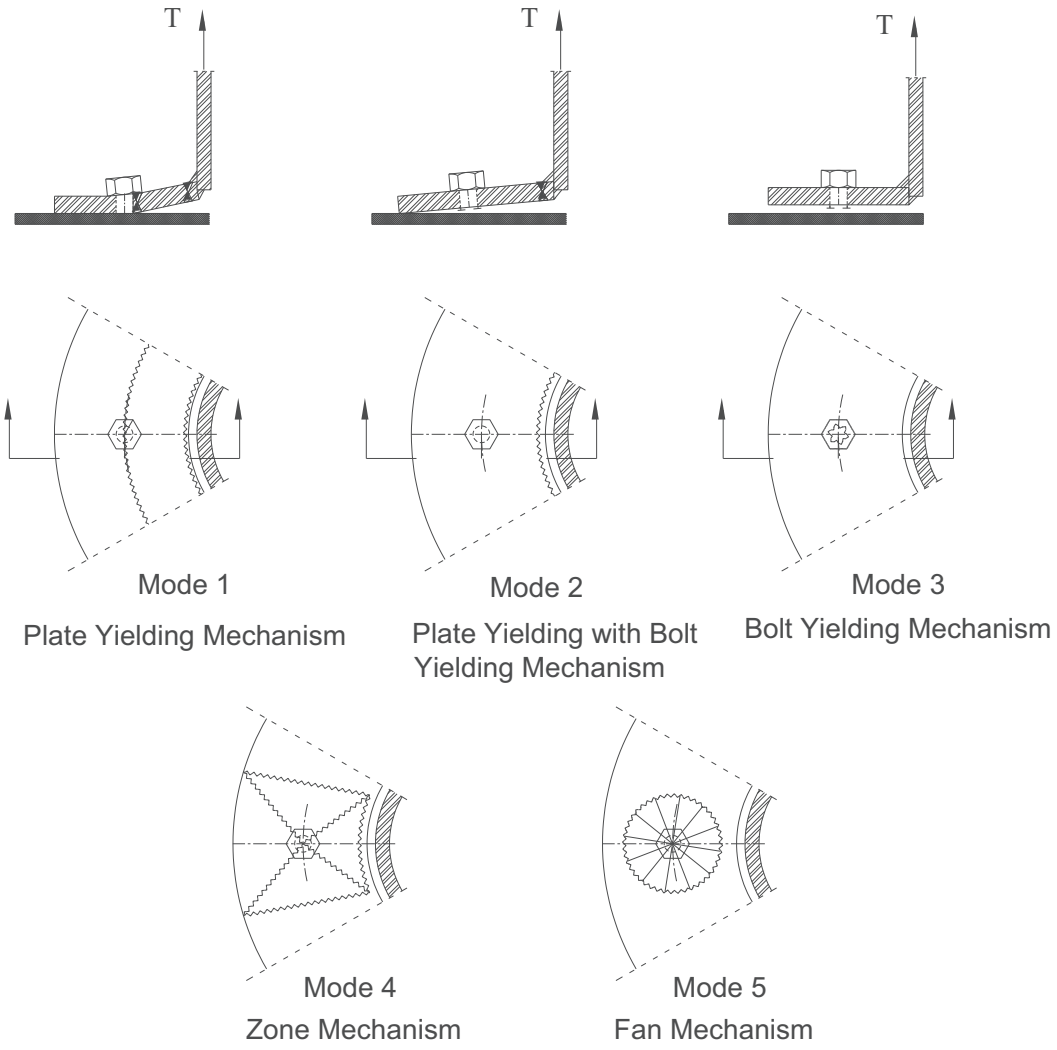

Fig. 6. Simplified failure mechanisms – yield line representations.

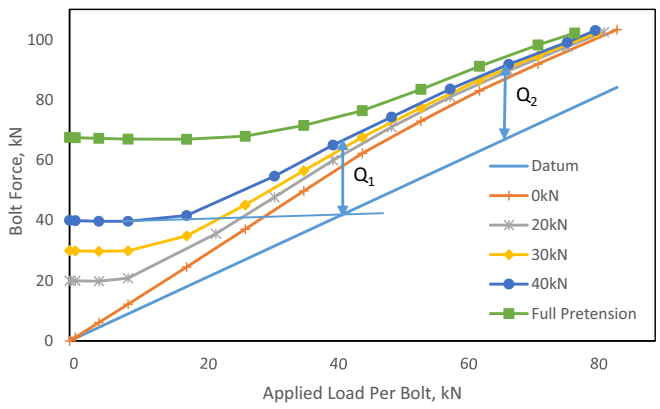

Fig. 7. Applied load per bolt vs bolt force for different pretension levels.

telecommunication and transmission applications which is chosen as 4″, 6″ or 8″. The other varied design parameters are:

1. Flange plate thicknesses: 8, 12, 15, 19 and 25 mm
2. Number of bolts: 4, 6 and 8

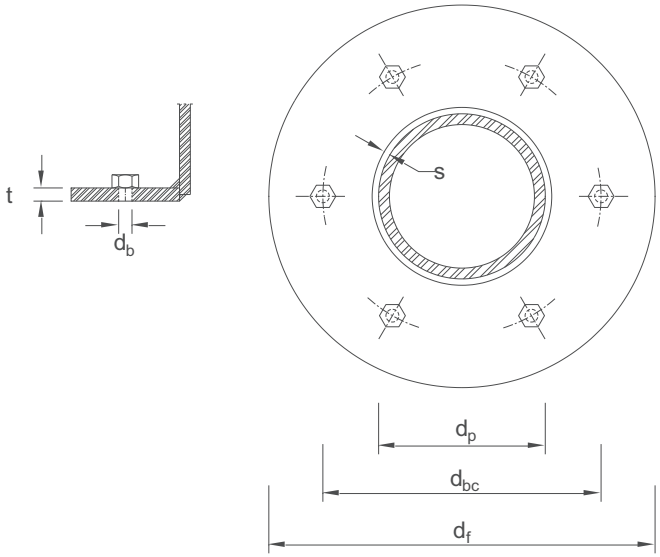

Fig. 8. Connection outline and design parameters.

Table 1
Finite element analysis calculated yield loads and associated modes of failure.

(a) 4" Diameter Pipe Connections

Specimen	Plate Thickness, mm	No. of Bolts	BC Diameter, mm	Plate Diameter, mm	ADINA Yield Load, kN	Failure Mode
4-01	8				192	Zone
4-02	12				279	Plate & Bolt
4-03	15				366	Bolt
4-04	19				366	Bolt
4-05	25	4	162	210	366	Bolt
4-06	8				299	Plate
4-07	12				410	Plate & Bolt
4-08	15				480	Plate & Bolt
4-09	19				550	Bolt
4-10	25	6	162	210	550	Bolt
4-11	8				256	Plate
4-12	12				477	Plate
4-13	15				513	Plate & Bolt
4-14	19				661	Plate & Bolt
4-15	25	8	162	210	740	Bolt
4-16	8				129	Plate
4-17	12				199	Zone
4-18	15				230	Plate & Bolt
4-19	19				289	Plate & Bolt
4-20	25	4	216	264	374	Bolt
4-21	8				128	Plate
4-22	12				248	Plate
4-23	15				299	Plate
4-24	19				384	Plate & Bolt
4-25	25	6	216	264	513	Plate & Bolt
4-26	8				128	Plate
4-27	12				283	Plate
4-28	15				367	Plate & Bolt
4-29	19				427	Plate & Bolt
4-30	25	8	216	264	555	Plate & Bolt
4-31	8				98	Plate
4-32	12				150	Plate & Bolt
4-33	15				170	Plate & Bolt
4-34	19				213	Plate & Bolt
4-35	25	4	267	315	300	Plate & Bolt
4-36	8				103	Plate
4-37	12				192	Plate
4-38	15				213	Plate & Bolt
4-39	19				256	Plate & Bolt
4-40	25	6	267	315	341	Plate & Bolt
4-41	8				103	Plate
4-42	12				214	Plate
4-43	15				235	Plate & Bolt
4-44	19				307	Plate & Bolt
4-45	25	8	267	315	422	Plate & Bolt

(b) 6" Diameter Pipe Connections

Specimen	Plate Thickness, mm	No. of Bolts	BC Diameter, mm	Plate Diameter, mm	ADINA Yield Load, kN	Failure Mode
6-01	8				210	Zone
6-02	12				361	Plate & Bolt
6-03	15				367	Bolt
6-04	19				370	Bolt
6-05	25	4	216	265	370	Bolt
6-06	8				300	Zone
6-07	12				452	Plate & Bolt
6-08	15				506	Plate & Bolt
6-09	19				542	Bolt
6-10	25	6	216	265	550	Bolt
6-11	8				325	Plate
6-12	12				542	Plate & Bolt
6-13	15				599	Plate & Bolt
6-14	19				723	Bolt
6-15	25	8	216	265	734	Bolt
6-16	8				132	Zone
6-17	12				226	Plate & Bolt
6-18	15				271	Plate & Bolt
6-19	19				362	Bolt
6-20	25	4	267	315	367	Bolt
6-21	8				168	Plate
6-22	12				289	Plate & Bolt
6-23	15	6	267	315	362	Plate & Bolt

(*continued on next page*)

Table 1 (*continued*)

(b) 6" Diameter Pipe Connections

Specimen	Plate Thickness, mm	No. of Bolts	BC Diameter, mm	Plate Diameter, mm	ADINA Yield Load, kN	Failure Mode
6-24	19				452	Plate & Bolt
6-25	25				550	Bolt
6-26	8				163	Plate
6-27	12				362	Plate & Bolt
6-28	15				398	Plate & Bolt
6-29	19				500	Plate & Bolt
6-30	25	8	267	315	633	Plate & Bolt
6-31	8				100	Zone
6-32	12				170	Zone
6-33	15				203	Zone
6-34	19				271	Plate & Bolt
6-35	25	4	321	369	370	Bolt
6-36	8				118	Plate
6-37	12				213	Plate & Bolt
6-38	15				235	Plate & Bolt
6-39	19				317	Plate & Bolt
6-40	25	6	321	369	452	Plate & Bolt
6-41	8				125	Plate
6-42	12				260	Plate & Bolt
6-43	15				316	Plate & Bolt
6-44	19				362	Plate & Bolt
6-45	25	8	321	369	497	Plate & Bolt

(c) 8" Diameter Pipe Connections

Specimen	Plate Thickness, mm	No. of Bolts	BC Diameter, mm	Plate Diameter, mm	ADINA Yield Load, kN	Failure Mode
8-01	8				210	Zone
8-02	12				367	Bolt
8-03	15				370	Bolt
8-04	19				370	Bolt
8-05	25	4	267	315	370	Bolt
8-06	8				288	Zone
8-07	12				494	Plate & Bolt
8-08	15				550	Bolt
8-09	19				550	Bolt
8-10	25	6	267	315	550	Bolt
8-11	8				411	Zone
8-12	12				576	Plate & Bolt
8-13	15				658	Plate &Bolt
8-14	19				734	Bolt
8-15	25	8	267	315	734	Bolt
8-16	8				135	Zone
8-17	12				226	Plate & Bolt
8-18	15				329	Plate & Bolt
8-19	19				370	Bolt
8-20	25	4	321	369	370	Bolt
8-21	8				198	Zone
8-22	12				296	Plate & Bolt
8-23	15				395	Plate & Bolt
8-24	19				484	Plate & Bolt
8-25	25	6	321	369	545	Bolt
8-26	8				200	Plate
8-27	12				346	Plate & Bolt
8-28	15				470	Plate & Bolt
8-29	19				590	Plate & Bolt
8-30	25	8	321	369	730	Bolt
8-31	8				107	Zone
8-32	12				185	Plate & Bolt
8-33	15				226	Plate & Bolt
8-34	19				330	Plate & Bolt
8-35	25	4	372	420	370	Bolt
8-36	8				144	Plate
8-37	12				228	Plate & Bolt
8-38	15				288	Plate & Bolt
8-39	19				370	Plate & Bolt
8-40	25	6	372	420	535	Plate & Bolt
8-41	8				144	Plate
8-42	12				288	Plate & Bolt
8-43	15				308	Plate & Bolt
8-44	19				411	Plate & Bolt
8-45	25	8	372	420	617	Plate & Bolt

3. Bolt circle diameter: pipe diameter plus 3 bolt diameters, next pipe diameter plus 3 bolt diameters and subsequent pipe diameters plus 3 bolt diameters
4. Outer plate diameter: bolt circle diameter plus 3 bolt diameters

While individually varying the above listed parameters, the following parameters are kept unchanged: steel material used yield stress of $f_y = 350$ MPa and a tensile strength $f_u = 450$ MPa; bolts are 5/8″ in diameter having grade F3125-A325 and the weld metal is chosen to match that of the flange plate.

As the focus of this study is primarily on the flange plate and/or bolts failure, the pipe wall thickness and outer and inner weld sizes are designed not to fail before the other connection components.

Fig. 8 shows general outline of the connection with the varying design parameters identified on the drawing.

ADINA software is used to perform a total of 135 analyses resulting from varying the design parameters. From each of these analyses the load vs displacement and load vs bolt force curves are plotted in order to determine the yield load. Several methods have been proposed for determining the resistance of a steel joint such as ECCS method. Using the ECCS method, the connection resistance is located at the intersection of the initial slope of the load displacement curve of the connection under investigation and tangent with one tenth slope to the that curve [20]. When the plotted load displacement curve does not follow the general shape suitable for the use of the ECCS method the connection resistance is determined using either the applied load vs bolt force blotted curve similar, by investigation or both. For each of the 135 models, the yield load and the failure mode are determined and listed in Table 1. It should be noted that for the range of the geometries covered in this parametric study the fan mechanism is not identified as the cause of yielding for any of the connections.

5. Yield line analysis

The yield line method was developed in the sixties of the previous century to calculate the ultimate strength of reinforced concrete slabs. Yield line method is based on the principle of virtual work where a solution is found by virtually equating the internal work required to accomplish the plastic deformation of a connected material to the virtual work performed by moving the load through a distance compatible with the deformation of the connected material called external work[10,19]. To be able to find the yield load, yield line method requires the failure pattern to be known in priori. Many yield line patterns may be valid for a given joint configuration. Since the resulting yield load is an upper bound solution, it is therefore necessary to find the pattern that gives the lowest load which provides results closest to the true yield load. Therefore, selection of the proper yield line pattern is of utmost importance as the choice of incorrect yield line pattern will produce unsafe results [1,4].

Yield line analysis was used in numerous studies to evaluate capacities of several joint configurations under different loading conditions [4–6,12,17,18].

To apply the principle of yield line to the circular flange plate connection under investigation it is crucial to first make proper assumptions of the location of plastic hinges and the pattern of the assumed yield lines. The external work done by the applied force is then calculated and equated to the internal work done by the rotation of the plates around the assumed yield lines.

The external work done is expressed as the applied tension load, T, multiplied by the displacement of the base plate at the interface with the pipe, δ, caused by this load:

$$W_e = T \times \delta \tag{1}$$

The internal work done is the sum of the work done by the formed yield lines under investigation:

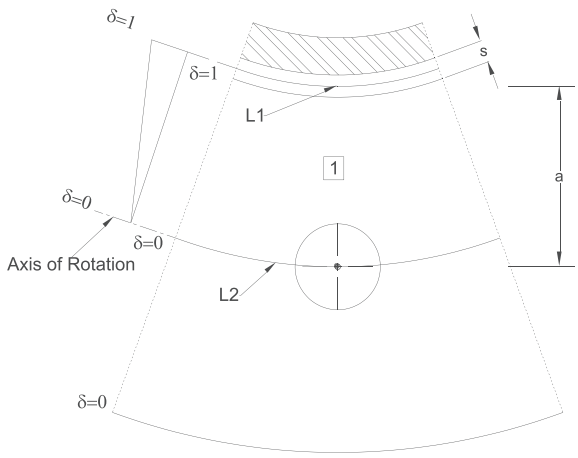

Fig. 9. Plate yielding mechanism.

$$W_i = \sum_{i=0}^{m} m_p \times L_i \times \theta_i \tag{2}$$

In the above equation:
m_p = plastic moment per unit length.
L_i = length of the yield line i.
θ_i = rotation yield line i.
i and m = yield line number and total number of yield lines respectively.

When yielding of the bolt group is introduced, eq. 2 is modified to include a term representing the work done by the bolts:

$$W_i = \sum_{i=1}^{m} m_p \times L_i \times \theta_i + n \times P_y \times \delta_b \tag{3}$$

Where:
P_y = bolt yield load.
n = number of bolts.
δ_b= displacement at bolt.
When only yielding of bolts occurs, eq. 3 is reduced to:

$$W_i = n \times P_y \times \delta_b \tag{4}$$

Where:
δ_b= displacement at bolt which in this case it is equal to δ.
In eqs. 2 and 3 above the plastic moment per unit length of yield line is calculated using the following equation:

$$m_p = f_y \times \frac{t^2}{4} \tag{5}$$

Where:
f_y = yield stress of the plate material
t = plate thickness
Whereas in eqs. 3 and 4 the bolt yield load is calculated using the following equation:

$$P_y = f_{yb} \times A_s \tag{6}$$

Where:
f_{yb} = yield stress of the bolt material
A_s = bolt stress or net cross-sectional area
The connection strength is then calculated by equating the external work done by the applied load and the internal work done by yield lines, yield lines and bolts, or bolts.

$$W_e = W_i \tag{7}$$

Eq. 7 is used considering all five possible failure mechanisms from which the minimum internal work is determined then the connection strength is calculated.

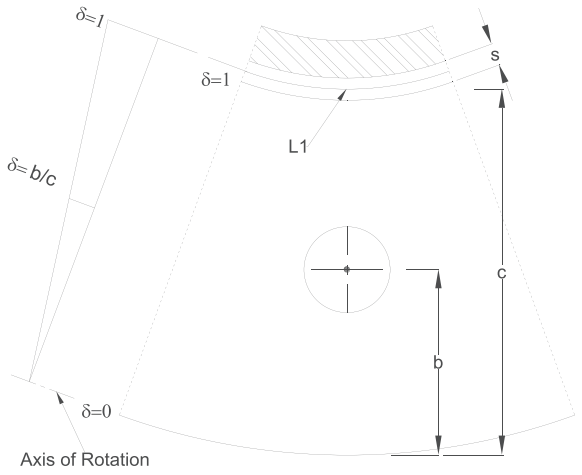

Fig. 10. Yielding around the pipe associated with bolt group yielding.

5.1. Plate yielding mechanism, mode 1

Plate yielding mechanism assumes that two circular yield lines are formed in the plate as shown in Fig. 9. In this mechanism the yield line formed around the pipe perimeter, L_1, is assumed to be located half weld size from the pipe wall while the second yield line, L_2, is assumed to coincide with the bolt circle.

In this case the internal work done by the plate is calculated by:

$$W_i = \pi \times m_p \times \left(d_p + s + d_{bc}\right) \times \frac{\delta}{a} \tag{8}$$

In the above equation:
d_p = pipe diameter
s = outer weld size
d_{bc}= bolt circle diameter
a= distance between the two yield lines

Using eq. 7 the tension force that causes this yield mechanism is determined from:

$$T_1 = \pi \times m_p \times \left(d_p + s + d_{bc}\right) \times \frac{1}{a} \tag{9}$$

5.2. Plate yielding associated with bolt yielding mechanism, mode 2

Fig. 10 shows the simplified yield line, displacement and rotation when yielding of the flange plate around the pipe perimeter occurs at the same instance as yielding of the bolt group. The length of the formed yield line in this case measured at have weld leg or $s/2$, L_1, undergoes a rotation while the group of bolts undergo elongation. The internal work done can then be expressed as:

$$W_i = \pi \times m_p \times \left(d_p + s\right) \times \frac{\delta}{c} + n \times P_y \times \frac{\delta \times b}{c} \tag{16}$$

After equating external work to internal work, the tension force that causes this mechanism is determined from:

$$T_2 = \pi \times m_p \times \left(d_p + s\right) \times \frac{1}{c} + n \times P_y \times \frac{b}{c} \tag{17}$$

5.3. Bolt yielding, mode 3

Although this mode of failure does not fit under yield line, it is included here to follow the sequence of failure modes presented in Fig. 6. In this mode of failure, the connection encounters yielding of the group of bolts without any yielding of the flange plate. In this case on the group of bolts contributes to the internal work which is given by:

$$W_i = n \times P_y \times \delta \tag{18}$$

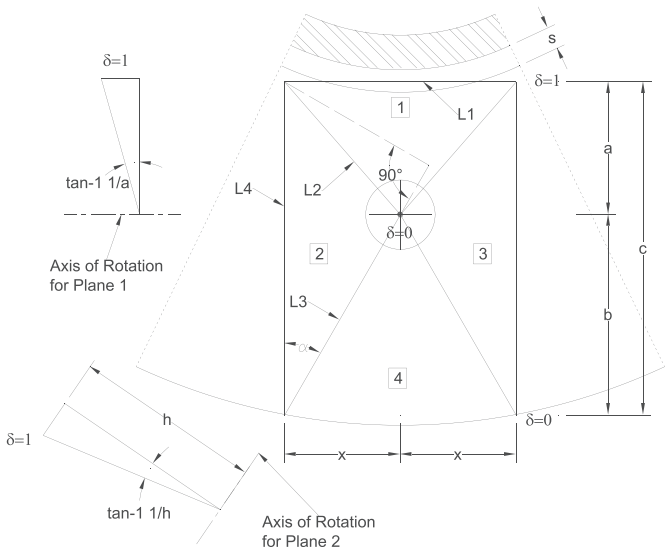

Fig. 11. Yield line mechanism for the localized zone failure mode.

And the external force that will cause this mode to occur is given by:

$$T_3 = n \times P_y \tag{19}$$

Due to the deformation of the flange plate bolts do not only elongate but bend as well, this is specially the case for relatively thin plates. This may be accounted for by reducing the bolt yield stress to account for the additional bending stresses. In this work however since bolt yielding is typically associated with thicker flange plates reduction in bolt yield stress is not considered.

5.4. Zone yielding mechanism, mode 4

Larger diameter pipes with fewer bolts will result in large circumferential spacing between bolts that in turn will make it easier for a local mechanism around each bolt to develop. Fig. 11 shows the simplified yield line mechanism associated with forming a zone mechanism in the flange plate. Four distinct planes are identified and numbered 1 through 4. Out of these four planes, planes 2 and 3 are symmetrical about an axis passing through the centre of the bolt hole and pipe while plane 4 is stationary.

Assuming the width of the zone is variable and equals $2\times$ the total

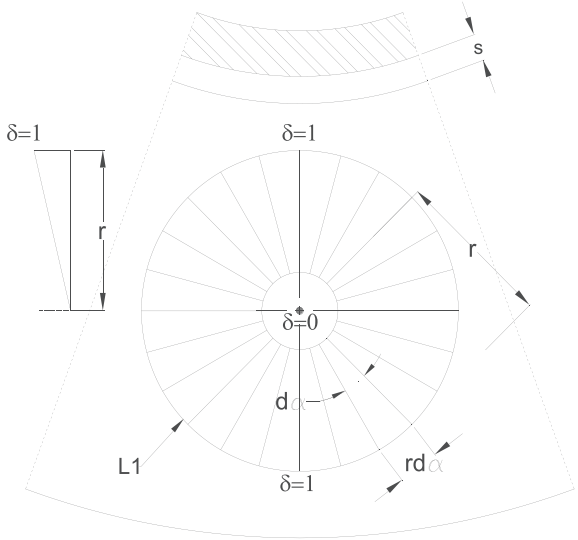

Fig. 12. Yield line associated with fan mechanism.

internal energy required to form this mechanism can be expressed in term of x as discussed below.

From the geometry of the zone and plane 1 the projection of yield lines L_1 and L_2 along the axis of rotation, $L_{1\&2}$, is given by:

$$L_{1\&2} = 4 \times x \tag{10-a}$$

And the rotation the above component undergoes, θ_1, is:

$$\theta_1 = \frac{\delta}{a} \tag{10-b}$$

For planes 2 and 3 and from the geometry of the zone, the component of L_2, L_3, and L_4 along the axis of rotation, $L_{2,3\&4}$, is given by:

$$L_{2,3\&4} = 2 \times (2 \times c \times cos\alpha) \tag{10-c}$$

And the rotation the above component. $\theta_{2\&3}$, undergoes is:

$$\theta_{2\&3} = \frac{\delta}{h} = \frac{\delta}{c \times sin\alpha} \tag{10-d}$$

From the above four equations the internal work required to form this zone mechanism is given by:

$$W_i = m_p \times \left(4 \times x \times \frac{\delta}{a} + 4 \times c \times cos\alpha \times \frac{\delta}{c \times sin\alpha}\right)$$

Which after simplifying yields the following internal work:

$$W_i = 4 \times m_p \times \left(x \times \frac{\delta}{a} + cos\alpha \times \frac{\delta}{sin\alpha}\right) \tag{10-e}$$

Substituting x variable by α from the geometry of the zone,

$$x = b \times tan\alpha \tag{10-f}$$

Eq. 10-e can then be re-written as:

$$W_i = 4 \times m_p \times \left(b \times tan\alpha \times \frac{\delta}{a} + cos\alpha \times \frac{\delta}{sin\alpha}\right) \tag{10-g}$$

The minimum required work for the flange plate to form this mechanism is then calculated by differentiating the internal work expression with respect to α and equating the result to zero which leads to:

$$\frac{dW_i}{d\alpha} = 0 = 4 \times m_p \times \delta \times \left(\frac{b}{a} \times \frac{d}{d\alpha}\left(\frac{sin\alpha}{cos\alpha}\right) + \frac{d}{d\alpha}\left(\frac{cos\alpha}{sin\alpha}\right)\right) \tag{11-a}$$

$$\frac{dW_i}{d\alpha} = 0 = 4 \times m_p \times \delta \times \left(\frac{b}{a} \times \left(\frac{cos\alpha \times cos\alpha + sin\alpha \times sin\alpha}{cos^2\alpha}\right) + \left(\frac{-sin\alpha \times sin\alpha - cos\alpha \times cos\alpha}{sin^2\alpha}\right)\right) \tag{11-b}$$

$$\frac{b}{a} \times \frac{1}{cos^2\alpha} = \frac{1}{sin^2\alpha} \tag{11-c}$$

$$tan\alpha = \sqrt{\frac{a}{b}} \tag{11-d}$$

Back substitute in eq. 10-f

$$x = b \times \sqrt{\frac{a}{b}} \tag{12}$$

Back substituting the value of α of in eq. 10-g and recognizing the fact that this is the work per bolt, the force that will cause the flange to form this mechanism is therefore:

$$T_4 = n \times 4 \times m_p \times \left(\frac{b}{a} \times \sqrt{\frac{a}{b}} + \sqrt{\frac{b}{a}}\right) \tag{13}$$

5.5. Fan mechanism, mode 5

Fan mechanism, Mode 5, may develop for pipes with large diameter and few bolts similar to zone mechanism. However, for fan mechanism to develop sufficiently large edge distance is also needed. . Fan mechanism, shown in Fig. 12, was studied previously [15] and the internal work done by the group of bolts associated with this mechanism is calculated by performing the integration presented in eq. 14:

$$W_i = n \times \int_0^{2\pi} 2r \times d\alpha \times \frac{\delta}{r} \times m_p \tag{14}$$

Using eq. 7 the tension force that cause this yield mechanism is determined from:

$$T_5 = n \times 4\pi \times m_p \tag{15}$$

This mechanism is referred to in the literature as punching or pull-through mechanism [4]. For this mechanism, prying force is theoretically zero.

5.6. Connection design and strength

In designing a circular flange connection, the number of bolts and bolt diameter d_b are chosen first followed by setting the bolt circle diameter d_{bc}. Bolt circle diameter should be set as small as possible while allowing acceptable clearance between the nut corner and the outside fillet weld which is recommended to be around 5 mm. The flange outside diameter is then selected such that the distance between flange edge and bolt circle diameter equals the distance between bolt circle diameter and pipe wall noting that flange diameter has negligible impact on the connection strength [8]. This is then followed by choosing a proper trial flange thickness, t, typically close to bolt diameter.

The connection strength, defined as the load causing yielding of the elements of the connection, is then determined by evaluating the forces T_1 through T_5. The minimum of these five calculated tension loads is the load at which the specimen will form a mechanism and yield which represents the connection resistance. It should be noted that it is recommended to avoid bolt group failure, therefore when such a failure is the controlling mechanism the connection design should be modified.

The calculated connection resistance load must then be compared to the applied tension load and the previous steps shall be repeated after changing the design parameters to obtain a safe, economical, and practical design.

6. Evaluation and discussion

The above expressions are used to calculate the yield loads and the associated modes of failure for the 135 connections geometries included in the parametric study and reported in Table 1. The purpose of performing these calculations is to evaluate the ability of these expression to accurately predict the yield load as well as to predict the associated mode of failure of flanged connections.

The validation is achieved through series of comparisons between the calculated yield loads and those obtained from the finite element analyses of the 135 connection geometries. The comparisons completed

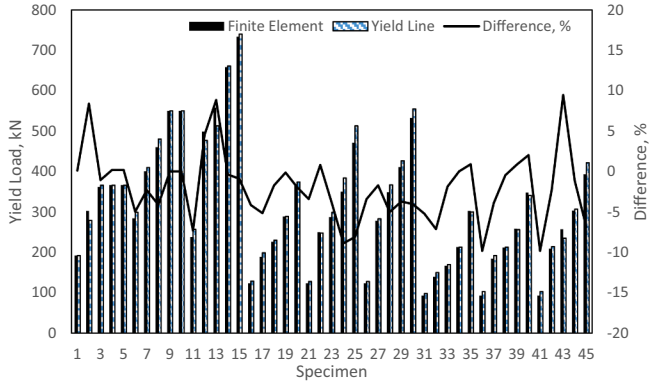

a) 4” Diameter Pipe

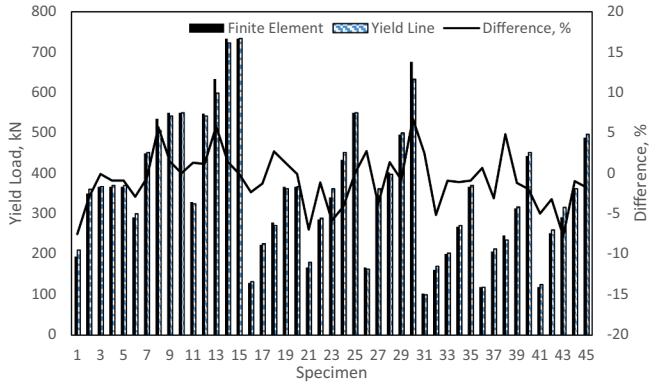

b) 6” Diameter Pipe

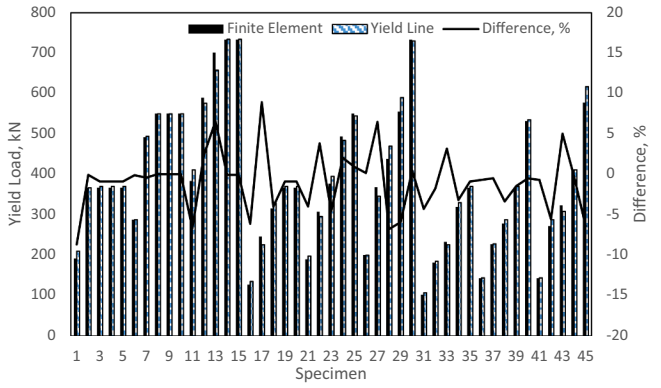

c) 8” Diameter Pipe

Fig. 13. Comparison between yield line analysis and ADINA predicted yield loads.

for the group of connections geometries listed in Table 1 are shown in Fig. 13 grouped by pipe diameter. In this figure, the left vertical axis is the yield load in kN while the right vertical axis is the difference between the ADINA predicted yield load and the calculated yield load as a percentage of the ADINA yield load. As can be seen from the figure the difference between the two values ranges from −10% to 9% with an average value of 2%.

Breaking down the difference by the controlling yield mechanism, or mode number, it is found that the difference for mode 1 ranges from −10% to 3%; for mode 2 ranges from −9% to 9%; for mode 3 ranges from −2% to 1% and for mode 4 ranges from 3% to 9%. The source of this error can be contributed to the approximate nature of the yield line analysis method and to the fact that the determination of the yield load

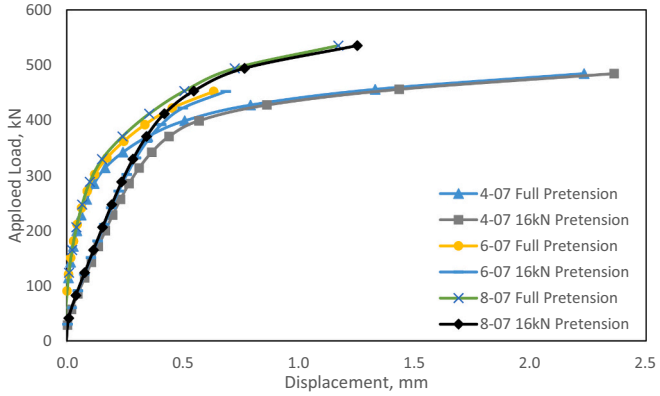

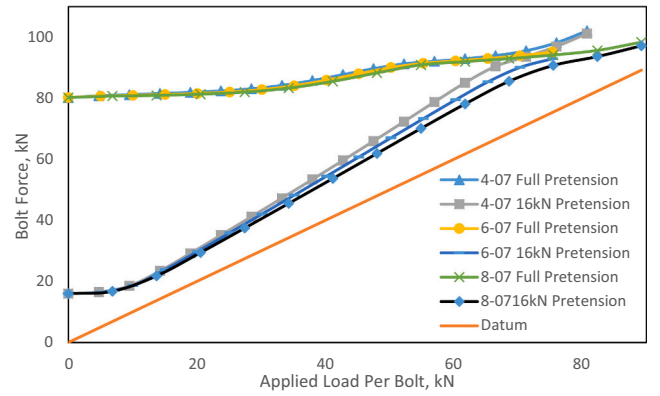

Fig. 14. Effect of bolt pretension force on displacement and failure load.

from FE analysis is achieved graphically from the load-deformation curve.

6.1. *Effect of bolt diameter and grade*

Although the parametric study and the validation of the proposed expressions focused only on 5/8″ bolts, it was not anticipated that the accuracy of the presented yield line expressions will be affected by the change of the bolt diameter or grade. This is also confirmed through performing several FE analyses of connections using different bolt diameters and grades. The resulting yield loads are then compared to the yield loads obtained from the yield line expressions and the calculated errors are found to be in the same range reported in parametric investigation for fully pretensioned bolts.

6.2. *Effect of number of bolts*

It is observed that that keeping all design parameters the same while increasing the number of bolts, the connection tends to yield in one of the two group-type mechanisms namely modes 1 and 2. Keeping all design parameters the same and decreasing the number of bolts, the connection tends to shift to single yield mode such as zone mechanism.

6.3. *Effect of plate thickness*

Connections with thin flange plates yield in either mode 1 or 4 depending, mainly, on the number of bolts. Increasing plate thickness shifts the failure mode to a combined plate and bolt yield mode, mode 2, further increasing the plate thickness shifts the failure mode to a bolt only failure mode, mode 3.

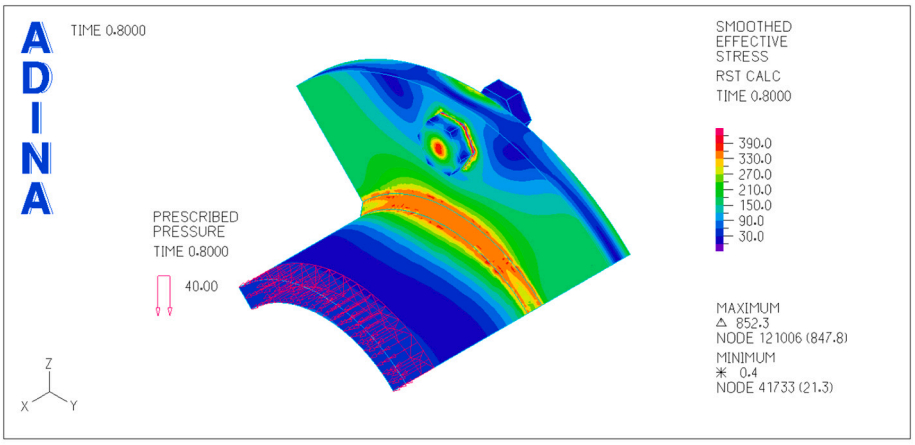

a) Full Bolt Pretension

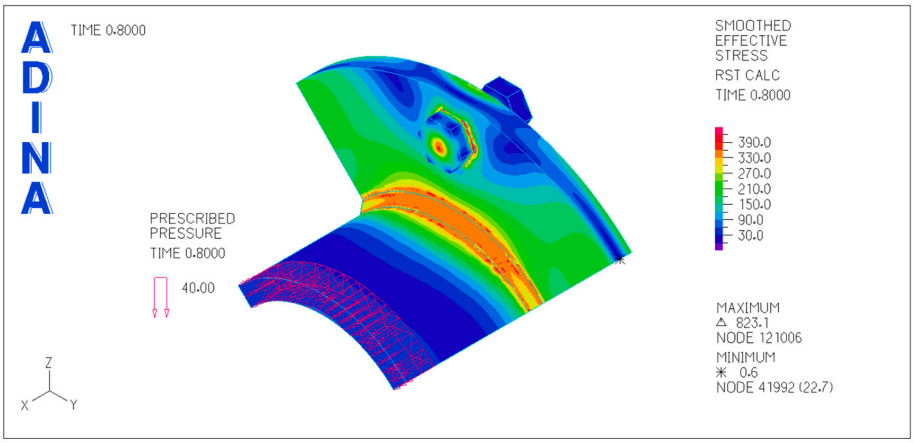

b) 16kN Bolt Pretension

Fig. 15. Effective stress distribution for two bolt pretension levels – specimen 6–17.

6.4. *Effect of bolt circle diameter*

In practice, truss members with pipe cross section typically connect to members with the same pipe diameter or one to two larger pipe diameters. Connecting to a larger pipe diameter translates into an increase in bolt circle diameter and in turn an increase in circumferential distance between bolts. From the study it is found that increasing the bolt circle diameter while keeping all other design diameter unchanged tends to shift the yield mechanism from a group type mechanism to individual mechanism. In addition, increasing bolt circle diameter move the yield mechanism from combined plate and bolt yielding mechanism to plate only yielding mechanism.

6.5. *Effect of bolt pretension load*

Design standards specify the necessity that bolts in joints to be installed to a specified minimum pretension load when subjected to tension load. In addition, it is considered a good practice not allowing the parts of tension loaded joint to separate under service load which dictates pre-tensioning the bolts. AISC, however, allows the use of snug tightened, 15–20% of the full pretension load, F3125-A325 bolt in joints subjected to static tensile loading [2,11].

Although, the current study does not focus on the effect of varying bolt pretension load has on flange plate connections under tension loads it is necessary to study this effect for the sole purpose of evaluating the accuracy of the proposed method. This is particularly useful as the presented yield line expressions are validated assuming bolts are fully pre tensioned. This effect is studied on one third of the connections included in the parametric investigation where bolt pretension load is lowered from full pretension to 16kNto gain insight on the effect this change has on the connection behaviour. Examining the results it is found, as anticipated, that connections with less pretension load exhibit a softer load displacement response when compared to connections with fully pretensioned bolts. Failure loads on the other hand remain at approximately the same level. Fig. 14 shows load displacement curve and load bolt force for specimens 4–07, 6–07 and 8–07 for the two levels of bolt pretension considered. Effective stress distribution for the two level of bolt pretension for specimen 6–17 is shown in Fig. 15 where the similarity between the contour line and stress levels are evident.

This confirms that the change in pretension load have little or no bearing on the connection yield load. It is also confirmed that varying pretension load does not change the yield mechanism. It is therefore concluded that the presented expressions can be used irrespective of bolt pretension load.

7. Conclusions

A numerical investigation of bolted circular flange plate connections behaviour under tension load is presented. The finite element software ADINA is used in the study implementing three dimensional solid elements, contact elements, bolt elements while considering material nonlinearities and contact-separation between bolts and flange plate as well as flange plate and contact surface. The finite element model assumptions are verified through series of comparisons between the predicted failure load and load displacement response and that of published test results. The model is found to predict accurately the reported failure load and load displacement response and is thus deemed satisfactory to be used in the study. The robustness of the model is also verified by altering the design variables and examining the model's ability to capture different failure modes as well as the development of the prying force in bolts.

A parametric investigation designed to capture the different anticipated yield mechanisms is then performed where design variables that include flange plate thickness, number of bolts, bolt circle diameter and flange plate diameter are varied to examine their effect on the connection behaviour.

The work progressed by presenting the different expected yield line mechanisms for the bolted flange plate bolted. The investigated mechanisms covered individual and group plate yielding, and plate and bolt yielding. As a result of this study simple close form expressions for the different yield line mechanisms are presented. The yield loads calculated based on these yield line expressions are then compared to the results of the finite element parametric investigation. Based on these comparisons it is concluded that the presented yield line expressions can predict the yield loads of the flange plate connections under tension with good accuracy.

Declaration of Competing Interest

The authors declare that they have no known competing financial interests or personal relationships that could have appeared to influence the work reported in this paper.

References

[1] T. Dranger, Yield line analysis of bolted hanging connections, Am. Inst. Steel Construct. Eng. J. (Third Quarter) (1977) 92–97.
[2] G.L. Kulak, High Strength Bolting for Canadian Engineers, Canadian Institute of Steel Construction, Willowdale, Ontario, Canada, 2005.
[3] ADINA Theory and Modelling Guide, ADINA 9.7, ADINA R&D Inc, Watertown, MA, 2021.
[4] B. Downswell, A yield line component method for bolted flange connections, Eng. J. (Second Quarter) (2011) 93–116.
[5] Y. Gong, Shear tab to hollow structural section column connections, Can. J. Civ. Eng. 41 (2014) 739–747.
[6] F. Karlsen, A. Aalberg, Bolted RHS end-plate joints in axial tension, in: Nordic Steel Construction Conference, Oslo, Norway, 5–7 September 2012, 2012.
[7] M.A. Khedr, S.A. Heikal, Finite element modelling of circular base plate connections, Ain Shams J. Civil Eng. 43 (1) (2009) 121–132.
[8] J.J. Cao, J.A. Packer, Design of tension circular flange joints in tubular structures, Eng. J. 34 (1) (1997) 17–25.
[9] B. Kato, R. Hirose, Bolted tension flanges joining circular hollow section members, J. Constr. Steel Res. 5 (1985) 79–101.
[10] R. Montuori, R. Muscatia, Plastic design of seismic resistant reinforced concrete frame, Earthquak. Struct. 8 (1) (2015) 205–224.
[11] G.L. Kulak, J.W. Fisher, J.H. Struik, Guide to Design Criteria for Bolted and Riveted Joints, American Institute of Steel Construction, Inc., Chicago, IL, USA, 2001.
[12] N. Kosteski, J.A. Packer, R.S. Puthli, A finite element method based yield load determination procedure for hollow structural section connections, J. Constr. Steel Res. 59 (2003) 453–471.
[13] M. Byfield, J. Davies, M. Dhanalakshmic, Calculation of the strain hardening behaviour of steel structures based on mill tests, J. Constr. Steel Res. 61 (2005) 133–150.
[14] M. Ghareeb, S. Heikal, M. Khedr, Design model for circular base plates under bending moment, Sci. Bull. 43 (1) (2008) 121–138. Faculty of Engineering, Ain Shams University. March.
[15] M. Couchaux, M. Hjiaj, I. Ryan, Static resistance of bolted circular flange joints under tensile force, in: Proceedings of the 13th international symposium on tubular structures, Hong Kong Vol. 1, 2010, pp. 27–35.
[16] H. Van-Long, J. Jean-Pierre, D. Jean-Francois, Behaviour of bolted flange joints in tubular structures under monotonic, repeated and fatigue loadings I: experimental tests, J. Constr. Steel Res. 84 (2013) 1–11.
[17] Y.Q. Wang, L. Zong, Y.J. Shi, Bending behavior and design model of bolted flange-plate connection, J. Constr. Steel Res. 84 (2013) 1–16.
[18] L. Massimo, R. Gianvittorio, D. Aldina, S. Luis, Experimental analysis and mechanical modeling of T-stubs with four bolts per row, J. Constr. Steel Res. 101 (2014) 158–174.
[19] E. Nastri, R. Montuori, V. Piluso, Seismic design of MRF-EBF dual systems with vertical links: EC8 vs plastic design, J. Earthq. Eng. 19 (3) (2015) 480–504.
[20] Couchaux, M., Hjiaj, M., Ryan, I. and Bureau, A. (2018). "Tensile resistance of bolted circular flange connections", Eng. Struct., Vol. 171, pp. 817-841.